Canadian Journal of Remote Sensing, 42:460–472, 2016

ISSN: 0703-8992 print / 1712-7971 online
DOI: 10.1080/07038992.2016.1229598

Taylor & Francis
Taylor & Francis Group

Introducing Close-Range Photogrammetry for Characterizing Forest Understory Plant Diversity and Surface Fuel Structure at Fine Scales

Benjamin C. Bright[1,*], E. Louise Loudermilk[2], Scott M. Pokswinski[3], Andrew T. Hudak[1], and Joseph J. O'Brien[2]

[1] *USDA Forest Service, Rocky Mountain Research Station, Forestry Sciences Laboratory, 1221 South Main Street, Moscow, ID 83843, USA*
[2] *USDA Forest Service, Southern Research Station, Center for Forest Disturbance Science, 320 Green Street, Athens, GA 30602, USA*
[3] *University of Nevada at Reno, 1664 North Virginia MS 0314, Reno, NV 89557, USA*

Abstract. Methods characterizing fine-scale fuels and plant diversity can advance understanding of plant-fire interactions across scales and help in efforts to monitor important ecosystems such as longleaf pine (*Pinus palustris* Mill.) forests of the southeastern United States. Here, we evaluate the utility of close-range photogrammetry for measuring fuels and plant diversity at fine scales (submeter) in a longleaf pine forest. We gathered point-intercept data of understory plants and fuels on nine 3-m^2 plots at a 10-cm resolution. For these same plots, we used close-range photogrammetry to derive 3-dimensional (3D) point clouds representing understory plant height and color. Point clouds were summarized into distributional height and density metrics. We grouped 100 cm^2 cells into fuel types, using cluster analysis. Comparison of photogrammetry heights with point-intercept measurements showed that photogrammetry points were weakly to moderately correlated to plant and fuel heights (r = 0.19–0.53). Mann–Whitney pairwise tests evaluating separability of fuel types, species, and plant types in terms of photogrammetry metrics were significant 44%, 41%, and 54% of the time, respectively. Overall accuracies using photogrammetry metrics to classify fuel types, species, and plant types were 44%, 39%, and 44%, respectively. This research introduces a new methodology for characterizing fine-scale 3D surface vegetation and fuels.

Résumé.. Les méthodes caractérisant les combustibles et la diversité végétale à fine échelle peuvent faire progresser la compréhension des interactions plantes-feux à plusieurs échelles et contribuer aux efforts pour surveiller les écosystèmes importants tels que les forêts de pin des marais (*Pinus palustris* Mill.) du sud-est des États-Unis. Ici, nous évaluons l'utilité de la photogrammétrie à courte distance pour mesurer les combustibles et la diversité des plantes à des échelles fines (de moins d'un mètre) dans une forêt de pins des marais. Nous avons recueilli des données de points d'interception des plantes de sous-bois et des combustibles sur 9 parcelles de 3 m^2 à une résolution de 10 cm. Pour ces mêmes parcelles, nous avons utilisé la photogrammétrie à courte distance pour dériver des nuages de points en 3 dimensions (3D) qui représentent la hauteur et la couleur des plantes de sous-bois. Les nuages de points ont été synthétisés en mesures simples pour les distributions de la hauteur et de la densité. Nous avons regroupé les cellules de 100 cm^2 en types de combustibles grâce à l'analyse par regroupement. La comparaison des hauteurs provenant de la photogrammétrie avec des mesures de points d'interception a montré que les points photogrammétriques étaient faiblement à modérément corrélés à la hauteur des plantes et des combustibles (r = 0,19 à 0,53). Les tests de Mann–Whitney par paire qui évaluent la séparabilité des types de combustibles, des espèces et des types de plantes en termes de mesures de photogrammétrie étaient significatifs 44%, 41%, et 54 % du temps, respectivement. Les précisions globales en utilisant les mesures de photogrammétrie pour classer les types de combustibles, les espèces et les types de plantes étaient de 44%, 39%, et 44 %, respectivement. Ces recherches présentent une nouvelle méthodologie pour la caractérisation de la végétation et des combustibles de surface à l'échelle fine en 3D.

INTRODUCTION

Quantifying the spatial structure and composition of forests has been vital for forestry and ecological applications throughout the last century. Data across large forested landscapes (10s km^2 to 1,000s km^2) are analyzed for wildlife habitat quality (Vierling et al. 2008; Smart et al. 2012), timber volume and yield (Murphy 2008), carbon quantification (Hudak et al. 2012), inputs to fire behavior models (Riano et al. 2003; Seielstad and Queen 2003; Mutlu, Popescu, Stripling, et al. 2008; Mutlu, Popescu, and Zhao 2008), and natural resource management in general (Hudak et al. 2009).

Received 15 October 2015. Accepted 10 August 2016.
*Corresponding author e-mail: benjamincbright@fs.fed.us

More recently, quantifying the structure of under- and mid-story vegetation has been of interest, given that heterogeneity in surface fuels, fire behavior, and plant community composition occurs at similarly fine scales (within a few meters; Kirkman et al. 2001; Loudermilk et al. 2012). Within longleaf pine (*Pinus palustris* Mill.) forests of the southeastern United States, measurement scale and feedbacks on multiscale community dynamics is critical (Mitchell et al. 2009). Here, the fire regime is of high frequency and low intensity where the understory, i.e., surface fuels, determine fire behavior patterns and processes (Hiers et al. 2009; Loudermilk et al. 2012), which is ultimately guided by the structure of the overstory (O'Brien et al. 2008; Mitchell et al. 2009) in determining fire effects on understory plant community assembly (Wiggers et al. 2013).

Quantifying and modeling vegetation or fuels at this fine scale is inherently difficult and prone to human error (Keane 2013). In the past, photogrammetry (using aerial imagery; Spurr 1960; United States Forest Service 1975), and more recently airborne laser scanning (ALS) have been used to quantify canopy structure (e.g., Andersen et al. 2005; Hudak et al. 2008), although less attention has been directed toward finer-scale understory data. Recently, Riano et al. (2007) estimated shrub height with ALS and infrared orthoimagery; Martinuzzi et al. (2009) classified shrub cover with ALS; and Hudak et al. (2015) predicted surface fuel loads with ALS. Although these studies have demonstrated the utility of ALS for predicting understory fuel and vegetation attributes, the spatial resolution of such estimates are coarser than submeter and can suffer from canopy obstruction or insufficient horizontal resolution (Slatton et al. 2004; Hudak et al. 2015).

Terrestrial laser scanning (TLS), for which the laser scanning instrument is positioned under the tree canopy, has provided a means for estimating fine-scale (cm^3) structure of individual understory plants (< 1 m height) and relating these estimates to their leaf area, biomass, and fuel type (Loudermilk et al. 2009; Rowell and Seielstad 2012). Furthermore, surface fuelbed structural characteristics have been used to predict submeter fire behavior measurements with high accuracy ($R^2 = 0.78$–0.88; Loudermilk et al. 2012), which was not formerly possible when using traditional fuel measurement techniques.

Although TLS instruments produce invaluable information, the instruments, processing time, and required peripherals are expensive and laborious (Dassot et al. 2011). The field of photogrammetry, developed in the 1930s, uses overlapping (aerial) photographs to create "stereophotos" that are 3-dimensional (3D). Photogrammetry has been employed throughout the last century for timber cruising (Spurr 1960; Slama et al. 1980), mapping land use and land cover change (Miller et al. 2000), and estimating tree and stand characteristics (Næsset 2002; Zagalikis et al. 2005). As ALS became more affordable and accessible around the turn of the century, it quickly took the place of photogrammetry. This high-accuracy laser technology, when flown over large (1,000s km^2) landscapes, provides unrivaled topographic maps and estimates of forest metrics that trump those of the traditional and ostensibly arduous photogrammetry techniques (Lefsky et al. 2002; Paine and Kiser 2012). Photogrammetry has, however, recently advanced (Miller et al. 2000; Zagalikis et al. 2005); digital imagery and photogrammetric software or workstations have replaced hard copy photographs and stereoscopes. Furthermore, photogrammetry has recently become competitive with ALS, producing high-quality 3D measurements of urban and forest structures, and for a fraction of the cost (Baltsavias 1999; Leberl et al. 2010; Bohlin et al. 2012; Dandois and Ellis 2013). Although the characterization of a heterogeneous surface fuelbed with TLS has been demonstrated (Loudermilk et al. 2009; Loudermilk et al. 2012; Rowell and Seielstad 2012), there is no previously known documentation of measuring surface fuels at fine scales using close-range photogrammetry.

Our objectives were to introduce and describe a close-range photogrammetric approach to measuring the 3D structure of understory vegetation and woody debris and to test the utility of photogrammetric points for distinguishing and predicting understory fuels and plant diversity. More specifically, we compared height data derived from close-range photogrammetry and field measurements of fuelbed depth and evaluated the utility of photogrammetry-derived data for separating and classifying 10-cm scale fuel types, plant species, and plant types.

METHODS

Study Area

The study area is located in Eglin Air Force Base (AFB) in northwestern Florida, where frequent prescribed surface fire has allowed longleaf pine forest to persist (Figure 1). Temperatures average 24°C and range from 5°C to 32°C. Annual rainfall averages 157 cm and falls mainly in summer. Topography is flat and

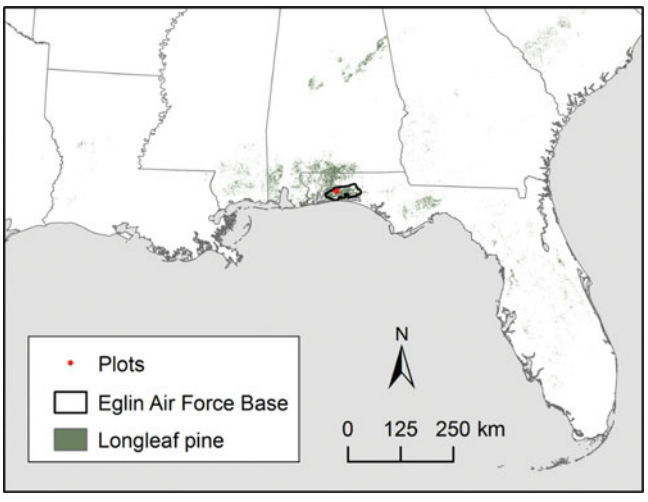

FIG. 1. Study plot locations and longleaf pine extent in Eglin Air Force Base (AFB), which is located in northwestern Florida (Ruefenacht et al. 2008).

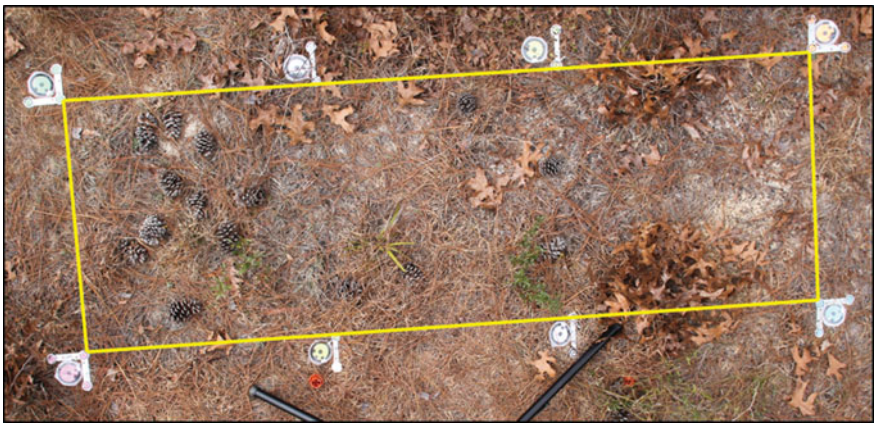

FIG. 2. Example of plot setup using strong ties, nails, and photogrammetry software printed (circular) targets. The yellow rectangle represents the approximate (1 m × 3 m) area that was cropped in the photogrammetry software for creating the stereo model.

soils are generally sandy (United States Air Force 2010). Eglin AFB sandhills are characterized as high pine by Myers and Ewel (1990) referring to the hilly undulating terrain dominated by an open longleaf pine canopy with a hardwood midstory made up of turkey oak (*Quercus laevis* Walter), blue jack oak (*Quercus incana* W. Bartram), and persimmon (*Diospyros virginiana* L.). Groundcover species in the study area are dominated by grasses broom sedge (*Andropogon virginicus* L.), and little bluestem (*Schizachyrium scoparium* (Michx.) Nash). Our particular study area within Eglin AFB had not burned in 2 years.

Field Observations

Vegetation and fuel characteristics were gathered in 9 plots located in longleaf pine sandhill habitat at Eglin AFB in February 2014 (Figure 1). For consistency in the influence of overstory canopy structure on fuels, the plots were placed < 5 m away from one adult (> 10 cm DBH) pine, but more than 5 m away from any other adult pine. Pinecones were placed in plots for a different study. Plots measured 1 m by 3 m in size and were gridded into cells measuring 10 cm by 10 cm, so that each of the 9 rectangular plots contained 300 cells. Each plot has permanent monuments so that an aluminum frame with steel rods can be placed to delineate all 300 cells. For each cell, point intercept measurements of plant species and fuels were taken at a single point in the center of each cell by using a probe. Fuel measurements included fuel and litter depths (cm), and presence or absence of any fuel categories (Table 2) that came into contact with the probe. All individuals by species were recorded within each cell. A total of 57 different species were observed, with an average of 19 species per plot and a standard deviation of 6 species across plots.

Photogrammetry Data and Processing

We used a photogrammetry technique to characterize the understory fuelbed within each plot. The technique produces a 3D point cloud by creating a stereo model from 2 overlapping digital photographs. To achieve this, we first carefully aligned 8 strong ties (15 cm in length) 1 m apart along the outside border of each plot and secured these ties in the ground using 60d 15-cm nails (Figure 2). This allowed for the clear identification of plot edges and cropping of images; it served the added purpose of recording fire intensity with infrared cameras (see O'Brien et al. this issue). Bulls-eye-shaped targets created and printed from the photogrammetry software (below) were color-coded and placed along the border of each plot on the strong ties for referencing during the photogrammetric processing (Figure 2). These targets are specifically designed for use in the software to ensure pairing photos with high accuracy. Typically, 3 reference targets were sufficient to scale and orient the photos, but additional targets were useful to double check distances and angles within each plot. Paired near-nadir-angle photographs were taken above each plot, using a Nikon D3200 camera with an 18-mm lens angle. The camera was mounted on a bar on an extendable pole stand for optimum camera placement above the plot. To capture the entire plot within each image, the cameras were extended to approximately 4 m. Ground sampling distance at this range was approximately 1 cm–4 cm. The camera stand was physically moved over about 40 cm to 50 cm to take a paired photo, while taking care to include the entire plot in each photo. Photographs were taken during even lighting conditions, typically on cloudy days with calm winds, or at dusk or dawn.

Digital imagery was processed with photogrammetry software PhotoModeler Scanner.[1] Using the "Smart Match" feature-based method in the software, stereo pairs were created by automatically detecting and matching pixels of similar texture and color between overlapping paired images. Bundle adjustment was then performed to optimize stereo pairs for the creation of final stereo models. The targets placed along the plot borders were used to scale stereo models to real units. Then, 3D points were extracted from each stereo model at a mean point spacing of 5 mm–10 mm (except for Plot 1, where the defined

[1]Eos Systems, Inc., Vancouver, British Columbia, 2015.

TABLE 1
Photogrammetry metric names and descriptions, and the number and percentage of times (given in parentheses) each metric was significantly different between fuel types, species, and plant types, as determined by Mann–Whitney tests

Metric Name	Description	Fuel Type	Species	Plant Type
R_avg	Average red value	21 (27)	13 (62)	3 (30)
G_avg	Average green value	35 (45)	10 (48)	6 (60)
B_avg	Average blue value	36 (46)	6 (29)	8 (80)
min	Minimum height	23 (29)	7 (33)	3 (30)
max	Maximum height	54 (69)	9 (43)	8 (80)
avg	Average height	48 (62)	12 (57)	8 (80)
std	Standard deviation of height	48 (62)	8 (38)	7 (70)
ske	Skewness of heights	3 (4)	2 (10)	1 (10)
kur	Kurtosis of heights	3 (4)	0 (0)	1 (10)
p10	10th percentile of heights	40 (51)	12 (57)	7 (70)
p25	25th percentile of heights	47 (60)	13 (62)	7 (70)
p50	50th percentile of heights	47 (60)	13 (62)	8 (80)
p75	75th percentile of heights	47 (60)	12 (57)	8 (80)
p90	90th percentile of heights	50 (64)	9 (43)	8 (80)
d00	Percentage of returns 0 cm–1 cm in height	24 (31)	10 (48)	5 (50)
d01	Percentage of returns 1 cm–3 cm in height	36 (46)	9 (43)	4 (40)
d02	Percentage of returns 3 cm–5 cm in height	16 (21)	9 (43)	2 (20)
d03	Percentage of returns 5 cm–10 cm in height	26 (33)	7 (33)	2 (20)
d04	Percentage of returns 10 cm–20 cm in height	43 (55)	9 (43)	5 (50)
d05	Percentage of returns 20 cm–30 cm in height	45 (58)	9 (43)	7 (70)
d06	Percentage of returns 30 cm–50 cm in height	28 (36)	2 (10)	6 (60)

point spacing was much greater) to create a point cloud for each plot. Red-green-blue (RGB) values from oriented photographs were assigned to points; if the angle between the point normal and the camera view vector was $< 90°$ (i.e., if the point was visible on the oriented photograph), then the RGB value of the photograph was included in the mean RGB calculation of that point. No interpolation was performed. Occlusion was not an issue as first, the vegetation and debris (leaf litter, woody material) were sparse (e.g., Fig. 2) due to frequent consumption by prescribed fire. This particular area had 2 years of regrowth and debris accumulation since the last burn. Next, the height data were downsampled to 10 cm $\times$ 10 cm for comparison with field data, where any issues of occlusion were absent or minimal.

Points were classified as ground or nonground, and normalized to heights above ground with LAStools software (Isenburg 2015). The lasground tool uses an unsupervised iterative algorithm to classify points and has demonstrated good performance for ALS in natural environments (Isenburg 2015). Although unsupervised, the user can adjust step size, terrain, and airborne parameters that affect how ground points are classified. We tested parameter sensitivity by experimenting with different combinations of the mentioned lasground parameters. Because we had no way of validating which points were ground, parameter sensitivity was tested by comparing how different parameters affected the fit between photogrammetric maximum fuel heights and field-measured fuelbed depths. Fit was measured via correlation, mean bias error, and root mean squared error; we chose final lasground parameters that maximized correlation and minimized mean bias error and root mean squared error between field-measured fuelbed depth and photogrammetric maximum fuel heights. The same lasground parameters were used for all plots.

The lascanopy tool was then used to generate 21 metrics for each 10 cm by 10 cm cell (Table 1). Metric cells were coincident with point-intercept cells characterized in the field as described in the previous section.

Cluster Analysis to Define Fuel Types

Following the methodology of Dimitrakopoulos (2002) and Hiers et al. (2009), who defined fuel types via cluster analysis, a grouping of cells into fuel types by cluster analysis was performed. Because our point-intercept fuel data were both continuous (fuel and litter depth) and binary (presence/absence of fuels), we chose Gower's distance, which allows for the inclusion of both continuous and binary variables, to create the dissimilarity matrix for the cluster analysis (Gower 1971). To determine the best number of clusters, the NbClust package in R was used (Charrad et al. 2014; R Core Team 2014). When computationally expensive indices are excluded, the NbClust routine calculates the best number of clusters, based on 26 different indices, and recommends using the number of clusters that the

majority of the indices indicate. We determined the best number of clusters in which to group observations into fuel types with the "variance ratio criterion" of Caliński and Harabasz (1974).

Statistical and Classification Analysis

We tested if photogrammetry metrics were able to distinguish the clustered fuel types, the 7 most abundant species (*Andropogon virginicus* L. (ANDVIR), *Aristida mohrii* Nash (ARIMOH), *Chrysopsis gossypina* (Michx.) Elliott (CHRGOS), *Licania michauxii* Prance (LICMIC), *Pityopsis aspera* (Shuttlw. ex Small) Small (PITASP), *Schizachyrium scoparium* (Michx.) Nash (SCHSCO), and *Schizachyrium tenerum* Nees (SCHTEN)), and plant types (forb, grass, ground cover, shrub, and seedling) by performing Kruskal–Wallis and Mann–Whitney rank sum tests, using R software. Significant Kruskal–Wallis tests indicated that, for a given metric, a distribution of at least 1 group was significantly different from distributions of the other groups. Mann–Whitney tests gave more specific information about which fuel types, species, and plant types varied significantly for which metrics, indicating whether 2 metric distributions came from different population distributions. We applied Bonferroni corrections to Mann–Whitney tests to control for Type 1 error. Cells that contained more than 1 species were excluded from species and plant type analyses, which eliminated 40% of the data. Because significant Kruskal–Wallis and Mann–Whitney tests showed that photogrammetry metrics differed among fuel types, species, and plant types, we tested how effectively photogrammetry metrics could classify fuel types, species, and plant types by using Random Forest (version 4.6–10) classification in R (Breiman 2001). Random Forest classification analyses grew 500 trees and selected 4 variables at each node. Overall classification accuracy was computed as 100 minus the out-of-bag estimate of error rate. Overall quantity and allocation difference were calculated using the diffeR package in R (Pontius and Santacruz 2015).

RESULTS

Comparison of Field-Measured and Photogrammetric Heights

Data from 3D photogrammetry resulted in an average point density of 11,765 points m^{-2} and ranged from 10,839 points m^{-2}–12,692 points m^{-2}, with the exception of Plot 1, where point density was 67,776 points m^{-2} due to a difference in the defined point extraction density. We found that the fit between photogrammetric and field-measured heights was insensitive to lasground parameters. Correlation, mean bias error, root mean squared error, and relative root mean squared error between field-measured fuelbed depth and photogrammetric maximum fuel heights ranged from 0.19–0.53, −3.56 cm–1.22 cm, 6.70 cm–25.56 cm, and 99%–152%, respectively (Figure 3). Field-measured fuelbed depth and photogrammetric maximum height patterns and distributions matched well (Figures 3 and 4), although systematic discrepancies were apparent. Field-measured heights were often much greater than photogrammetric heights, especially in Plots 1, 2, and 3 (Figure 3). Field-measured height distributions had a greater frequency of lower heights than photogrammetric height distributions in Plots 1, 2, 4, 5, 6, and 7 (Figure 4).

Statistical and Classification Analyses

A majority of indices in the NbClust routine selected 13 as the best number of clusters to divide the fuel data into (Table 2). Grass and longleaf pine litter were the most common fuels. The majority of the cells were classified as either "sparse vegetation and litter" (41%) or "sparse vegetation and perched pine litter" (18%; *perched* meaning pine litter is resting on vegetation rather than the ground).

Every Kruskal–Wallis test, except that testing whether kurtosis of heights varied significantly between species, was significant. Mann–Whitney tests revealed 720 of 1638 possible (44%) significant differences in metric distributions between fuel types (Tables 1 and 3). Maximum, mean, and standard deviation of photogrammetry heights; height percentile metrics; and upper strata density metrics (d04, d05) were most often significantly different between fuel types (Table 1). Fuel types often varied significantly for >10 metrics, but were occasionally inseparable from one another. Fuel Type 8, defined as "sparse vegetation and litter," the most abundant fuel type, was the most separable. Fuel Type 12, defined as "grass and pine litter," was less separable than other fuel types.

Between species, 181 of 441 possible (41%) significant differences in metric distributions existed (Tables 1 and 4). Mean height, height percentile, and mean red value were most frequently significantly different between species (Table 1). ANDVIR was the most separable species, being highly separable from every other species. ARIMOH was the least separable, and was nearly or completely inseparable from PITASP, SCHSCO, and SCHTEN (Table 4). Other species were moderately separable, being separable from some species but inseparable from others. For example, CHRGOS was fairly separable from every other species except LICMIC.

For plant type, 114 of 210 possible (54%) significant differences in metric distributions were found (Tables 1 and 5). Similar to fuel types, maximum, mean, and standard deviation of photogrammetry heights; height percentile metrics; and d05 were most often significantly different between plant types (Table 1). Less separable plant type pairs included forb and ground species, grass and seedlings, and shrubs and seedlings (Table 5).

Despite significant Kruskal–Wallis tests and the large number of significant Mann–Whitney tests, fuel types, species, and plant types were fairly confused when all 21 photogrammetry metrics were used as predictors in classification analyses. Overall classification accuracies of fuel type, species, and plant

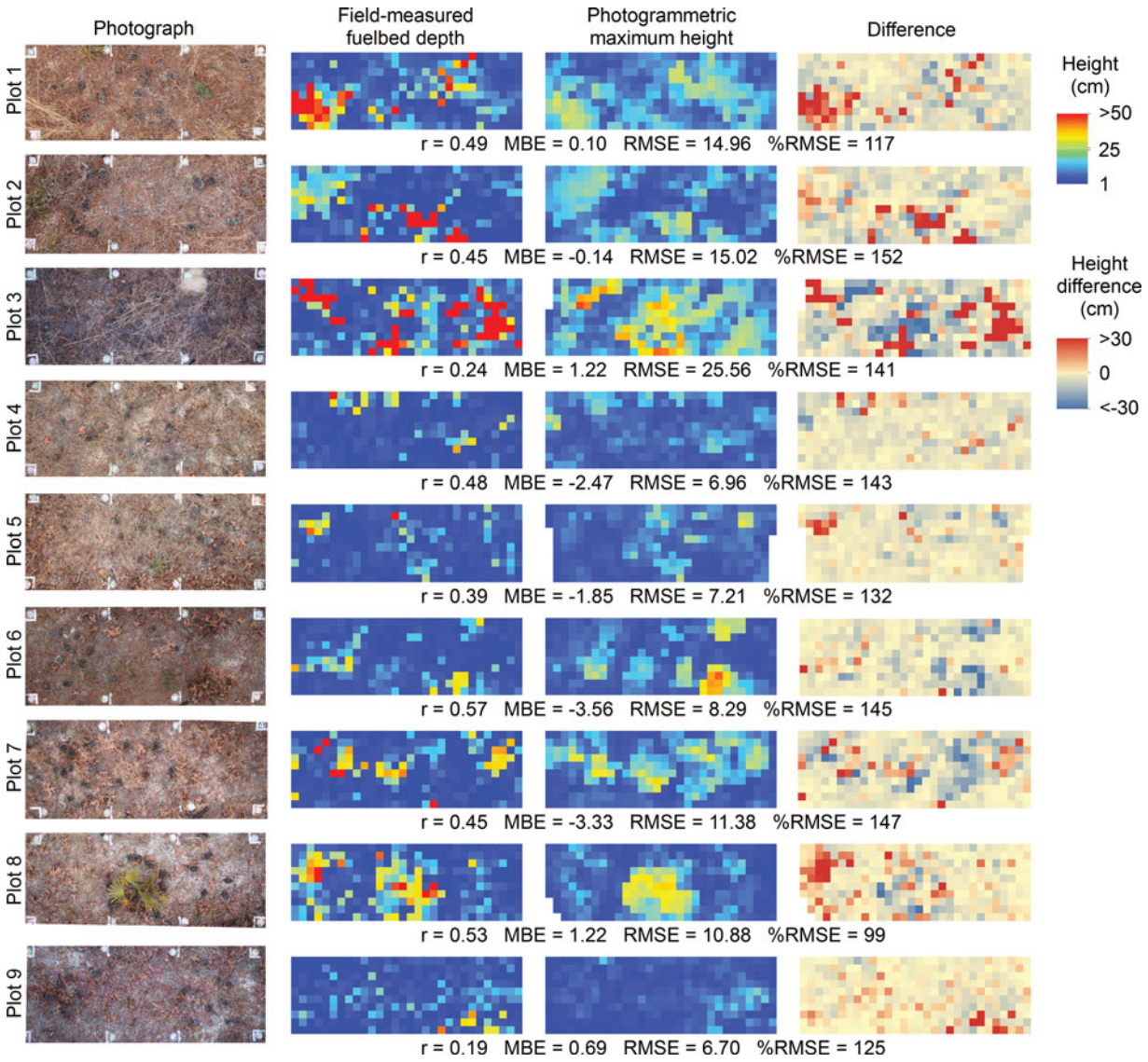

FIG. 3. Comparisons of true-color photographs, field-measured fuelbed depth, photogrammetric maximum fuel height for each plot, and the difference (field-measured fuelbed depths minus photogrammetric maximum fuel heights).

type classifications were 44%, 39%, and 44%, respectively (Tables 6–8). Confusion between classes revealed by Mann–Whitney tests were reflected in classification analyses, although the number of observations of each fuel type, species, and plant type had a large influence on classification accuracy that furthered confusion; commission errors were greater and omission errors were fewer for fuel types, species, and plant types with more observations, and vice versa. For example, the most abundant species, LICMIC, had the smallest omission error rate, 34%, but the largest commission error rate, 86%. Although Mann–Whitney tests showed that ANDVIR was highly separable from all other classes, it was frequently classified as LICMIC simply because of the large number of observations of LICMIC (Table 7). For the fuel type classification, the most abundant fuel types, 8 and 9, were also the most separable as determined by the Mann–Whitney test. However, because they were much more abundant than other classes, they still had the highest commission error rates, 61% and 72%, respectively (Table 6).

DISCUSSION

We found that photogrammetry is applicable for characterizing surface fuelbeds and predicting plant types. Although photogrammetry has been used for 3D depiction of overstory trees (Dandois and Ellis 2013; Lisein et al. 2013), this is the first demonstration of using photogrammetry for characterization of fine-scale understory fuels and plants. Loudermilk et al. (2009) showed that fine-scale TLS metrics were correlated with

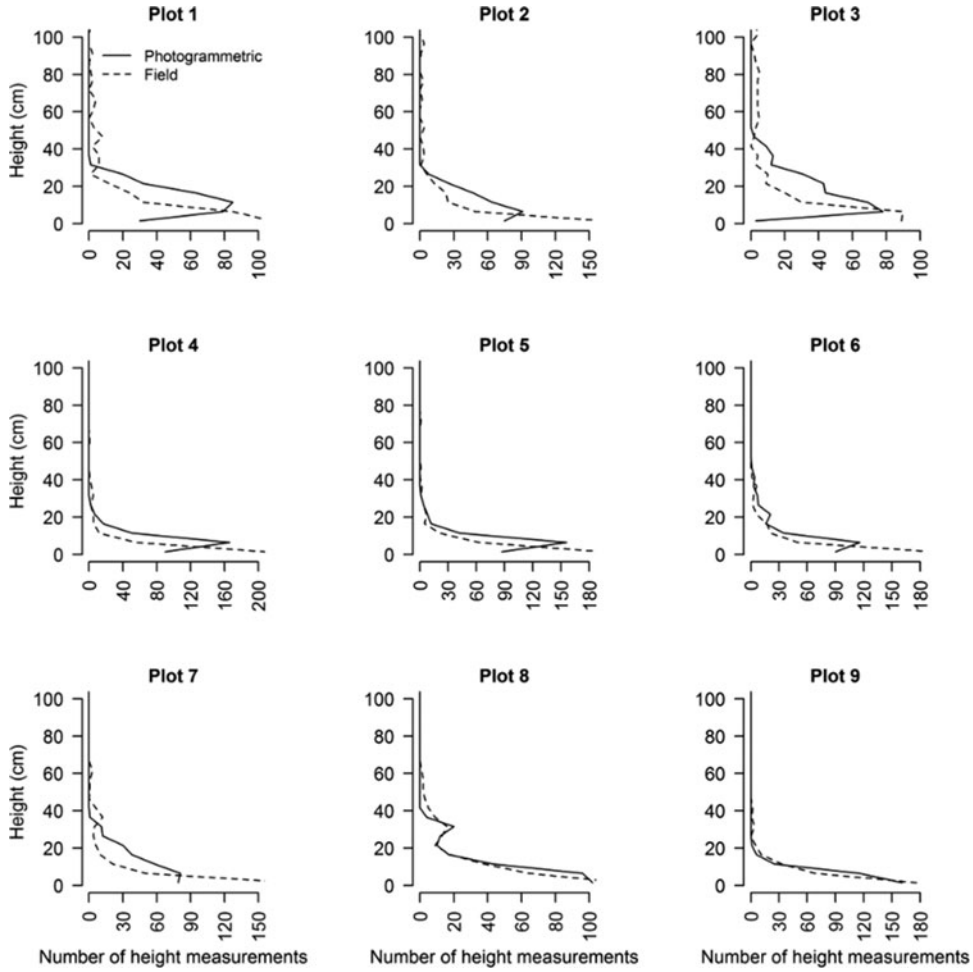

FIG. 4. Distributions of 300 photogrammetric maximum heights and 300 fuelbed depths derived from point-intercept measurements for each plot.

understory biomass and captured understory height variation better than point-intercept sampling; Loudermilk et al. (2012) found that height metrics generated from TLS could be used to predict fire behavior at fine scales. Fine-scale height metrics produced using photogrammetry, such as those produced here, might also be effective predictors of fire behavior; future research could evaluate this capability.

To evaluate the ability of photogrammetry to approximate point-intercept data, we compared point-intercept measurements of fuelbed depth to maximum photogrammetry height because this metric was the best approximation of measured fuelbed depth. In our case, parameters for normalizing point-cloud heights that we optimized based on field measurements were insensitive, and normalizing point-cloud heights using the default lasground parameters yielded nearly identical results. Thus, our approach does not necessitate the inclusion of field-measured height information for parameterization of point-cloud height normalization. Still, we recommend taking some field height measurements so that accurate height normalization can be verified. Point-intercept data is not necessarily the best or most accurate representation of understory fuels and plants. In fact, photogrammetry and TLS yield much more height information than traditional point-intercept measurements, thereby capturing height variation at finer scales than point-intercept measurements are able to capture. We were able to take 300 point-intercept measurements of fuelbed depth for each plot, whereas photogrammetry resulted in tens of thousands of height measurements for each plot. Photogrammetry and TLS height information is also less subjective and less prone to human error than point-intercept measurements.

Patterns and distributions of point-intercept measurements of fuelbed depth and photogrammetric maximum height were similar, but there were discrepancies (Figures 3 and 4). Some spatial registration differences existed between the 2 datasets, i.e., a notable point-intercept measurement for $cell_{i,j}$ was located at times in an adjacent cell in the photogrammetry dataset. Some differences existed because point-intercept measurements and photogrammetry data were acquired at different times, so that

TABLE 2

Mean values of fuel categories for fuel types as determined by cluster analysis. Mean values are expressed as percentages, except for litter and fuel depths where mean depth in cm is given. Presence and absence of each fuel category was measured for each 100 cm^2 cell. Wiregrass (*Aristida stricta* Michx., *A. beyrichiana* Trin. & Rupr.) and evergreen oak litter were also potential fuel categories but never occurred on plots

Fuel Type (N)	Litter Depth (Cm)	Fuel Depth (Cm)	1 Hour–10 Hour Fuels (%)	100 Hour–1,000 Hour Fuels (%)	Perched Pine Litter (%)	Perched Oak Litter (%)	Grass (%)	Shrubs (%)	Volatile Shrubs (%)	Forbs And Forb Litter (%)	Bare Soil (%)	Deciduous Oak Litter (%)	Longleaf Pine Litter (%)	Pinecone (%)
1. Perched pine and oak litter with grass and shrubs (15)	31	32	0	7	40	53	60	53	27	7	0	40	67	7
2. Flat pie and oak litter with pinecone (336)	1	5	4	21	2	0	67	9	4	8	1	28	45	21
3. Grass and pine litter with pinecone (22)	6	98	9	27	27	0	100	0	0	0	0	5	77	27
4. Volatile shrubs (104)	2	22	7	8	12	1	63	12	37	11	0	30	65	8
5. Grass and pine litter (41)	5	69	10	0	34	2	95	5	10	2	0	17	63	0
6. Shrubs, grass, and litter (119)	2	15	7	7	7	2	68	17	21	8	0	29	48	7
7. Shrubs, grass, and litter (83)	2	34	4	2	5	0	80	17	24	2	1	33	57	2
8. Sparse vegetation and litter (1088)	1	1	6	1	0	0	30	2	2	5	2	32	59	1
9. Sparse vegetation and perched pine litter (484)	4	5	6	10	27	2	46	3	4	4	0	38	75	10
10. Shrubs and perched pine litter (123)	12	13	6	18	89	4	44	7	22	7	0	22	76	15
11. Grass and shrubs (208)	2	10	7	13	8	1	72	15	14	13	0	31	48	13
12. Grass and pine litter (40)	4	49	10	3	18	0	93	5	18	5	0	28	65	3
13. Grass, volatile shrubs, and perched pine litter (16)	14	33	6	6	75	0	75	0	38	6	0	25	56	6

TABLE 3
Number and percentage of significant pairwise differences, as determined by Mann–Whitney tests, between fuel types in terms of photogrammetry metrics. A Bonferroni correction was applied to significance tests, so that p-values < 0.0038 (0.05/13) were considered significant. See Table 2 for fuel type descriptions

	1.	2.	3.	4.	5.	6.	7.	8.	9.	10.	11.	12.
1.												
2.	17 (81)											
3.	1 (5)	14 (67)										
4.	14 (67)	11 (52)	1 (5)									
5.	8 (38)	16 (76)	0 (0)	5 (24)								
6.	14 (67)	9 (43)	4 (19)	0 (0)	8 (38)							
7.	14 (67)	11 (52)	2 (10)	0 (0)	1 (5)	0 (0)						
8.	18 (86)	19 (90)	17 (81)	19 (90)	19 (90)	19 (90)	19 (90)					
9.	17 (81)	2 (10)	15 (71)	11 (52)	14 (67)	12 (57)	12 (57)	18 (86)				
10.	10 (48)	16 (76)	4 (19)	7 (33)	4 (19)	7 (33)	5 (24)	20 (95)	18 (86)			
11.	16 (76)	4 (19)	12 (57)	7 (33)	16 (76)	2 (10)	8 (38)	18 (86)	9 (43)	15 (71)		
12.	11 (52)	10 (48)	0 (0)	0 (0)	0 (0)	0 (0)	0 (0)	18 (86)	12 (57)	4 (19)	6 (29)	
13.	1 (5)	13 (62)	0 (0)	7 (33)	0 (0)	8 (38)	3 (14)	15 (71)	13 (62)	6 (29)	11 (52)	0 (0)

TABLE 4
Number and percentage of significant pairwise differences, as determined by Mann–Whitney tests, between species in terms of photogrammetry metrics. A Bonferroni correction was applied to significance tests, so that p-values < 0.00714 (0.05/7) were more conservatively considered significant

	ANDVIR	ARIMOH	CHRGOS	LICMIC	PITASP	SCHSCO
ANDVIR						
ARIMOH	12 (57)					
CHRGOS	14 (67)	10 (48)				
LICMIC	18 (86)	5 (24)	3 (14)			
PITASP	14 (67)	0 (0)	7 (33)	5 (24)		
SCHSCO	17 (81)	2 (10)	16 (76)	7 (33)	7 (33)	
SCHTEN	11 (52)	1 (5)	11 (52)	8 (38)	9 (43)	4 (19)

physical changes in fuels and plants (e.g., growth, trampled by fauna, wind, or other weather) could have occurred during that time. For some cells, photogrammetry maximum heights were much lower than point-intercept fuelbed depths (Plots 1–3 in Figure 3); in these cases, photogrammetry was unable to capture the heights of tall grass stems, which are arguably of little overall importance to understory fuels and resulting fire behavior. Photogrammetry can also suffer from occlusion, where objects block those underlying them.

TABLE 5
Number and percentage of significant pairwise differences, as determined by Mann–Whitney tests, between plant types in terms of photogrammetry metrics. A Bonferroni correction was applied to significance tests, so that p-values < 0.01 (0.05/5) were more conservatively considered significant

	Forb	Grass	Ground	Shrub
Forb				
Grass	14 (67)			
Ground	3 (14)	17 (81)		
Shrub	15 (71)	14 (67)	16 (76)	
Seedling	13 (62)	2 (10)	12 (57)	8 (38)

We have incorporated a recent advancement to the design (after this study) by using two identical cameras mounted about 50 cm apart on a parallax bar. Here, one can take 2 simultaneous photos in exactly the same lighting conditions to minimize vegetation change (mainly from wind) between photos. Although in pilot work capturing portions ($0.5\ m^2 - 1 m^2$) of the plot from different angles and distances from nadir was explored (Westoby et al. 2012; James and Robson 2013; Nouwakpo et al. 2015), we found that taking 2 photographs at nadir of the entire plot was important for reconstructing these fuels by standardizing light conditions, vegetation positions, and topography across the plot. Taking multiple pictures around the plot increased discrepancies of lighting between photos and created issues with merging data across the plot, where even slight (e.g., 1 cm) differences in topography or shifts in vegetation (from wind) could lower

TABLE 6
Confusion matrix of fuel type classification. Fuel types generated from cluster analysis were classified by using photogrammetry metrics. Overall accuracy, quantity difference, and allocation difference were 44%, 18%, and 38%, respectively

		Classification														
		1.	2.	3.	4.	5.	6.	7.	8.	9.	10.	11.	12.	13.	Total	Comm. Error (%)
Cluster Analysis	1.	**6**	1	0	1	0	1	2	0	2	0	1	1	0	15	40
	2.	0	**67**	1	1	0	6	2	162	65	10	21	1	0	336	51
	3.	0	1	**0**	1	1	5	0	5	6	1	2	0	0	22	23
	4.	1	10	1	**4**	0	11	3	29	23	9	12	1	0	104	29
	5.	1	3	1	1	**3**	1	1	6	12	5	6	1	0	41	32
	6.	1	13	1	9	0	**8**	3	47	25	8	4	0	0	119	39
	7.	0	5	1	6	0	3	**8**	31	12	6	6	4	1	83	29
	8.	1	51	0	1	2	5	3	**898**	106	5	14	2	0	1088	61
	9.	0	45	0	3	2	2	1	246	**152**	14	18	1	0	484	72
	10.	1	11	0	2	3	5	2	22	37	**29**	11	0	0	123	60
	11.	0	29	0	3	1	4	1	97	47	11	**13**	2	0	208	48
	12.	0	1	0	1	3	1	4	14	11	1	4	**0**	0	40	33
	13.	1	0	0	1	1	3	2	1	2	4	1	0	**0**	16	6
	Total	12	237	5	34	16	55	32	1558	500	103	113	13	1	2679	
	Omis. Error (%)	60	80	100	96	92	93	90	17	69	76	93	100	100		

quality of merged results. Although cloudy or dawn and dusk conditions are best, one can use a tarp or other method to create shade or even lighting conditions in full-sunlight conditions.

Our cluster analysis indicated that understory fuels were best separated into 13 classes; similarly, Hiers et al. (2009) found that 15 different fuel types provided a good representation of understory fuels in a similar longleaf pine ecosystem. Several of our fuel types correspond to those described in Hiers et al. (2009): flat pine and oak litter with pinecone (Fuel Type 2); grass and pine litter (Fuel Types 5 and 12); shrubs, grass and litter (Fuel Types 6 and 7); sparse vegetation and perched pine litter (Fuel Type 9); and shrubs and perched pine litter (Fuel Type 10). Forbs were more abundant on the plots of Hiers et al. (2009). Pinecones were artificially placed in our plots, and were therefore more prevalent in our plots than those of Hiers et al. (2009). Absent on our plots but fairly abundant in the plots of Hiers et al. (2009) was wiregrass (*Aristida stricta* Michx., *A. beyrichiana* Trin. & Rupr.). Wiregrass is more prevalent in the more productive longleaf pine forests of southwestern Georgia, where Hiers et al. (2009) worked, than at Eglin AFB (Noss 1989).

We found that metrics derived from photogrammetry data differed significantly among different fuel types, species, and

TABLE 7
Confusion matrix of species classification. Species measured in the field were classified using photogrammetry metrics. Overall accuracy, quantity difference, and allocation difference were 39%, 17%, and 44%, respectively

		Classification								
		ANDVIR	ARIMOH	CHRGOS	LICMIC	PITASP	SCHSCO	SCHTEN	Total	Comm. Error (%)
Ground Observation	ANDVIR	**33**	0	1	31	5	10	3	83	47
	ARIMOH	3	**4**	1	27	17	6	2	60	17
	CHRGOS	7	1	**3**	39	22	5	0	77	38
	LICMIC	13	2	10	**189**	23	45	5	287	86
	PITASP	4	4	11	44	**47**	31	4	145	68
	SCHSCO	5	2	5	90	17	**55**	2	176	64
	SCHTEN	7	1	1	15	14	2	**7**	47	34
	Total	72	14	32	435	145	154	23	875	
	Omis. Error (%)	60	93	96	34	68	69	85		

TABLE 8
Confusion matrix of plant type classification. Plant types measured in the field were classified using photogrammetry metrics. Overall accuracy, quantity difference, and allocation difference were 44%, 6%, and 50%, respectively

		Classification						
		Forb	Grass	Ground	Shrub	Seedling	Total	Comm. Error (%)
Ground Observation	Forb	**178**	141	75	0	0	394	58
	Grass	130	**211**	77	1	1	420	64
	Ground	89	111	**120**	0	0	320	50
	Shrub	0	6	1	**1**	0	8	13
	Seedling	8	11	6	0	**0**	25	4
	Total	405	480	279	2	1	1167	
	Omis. Error (%)	55	50	63	88	100		

plant types within a longleaf pine forest. However, despite significant differences, using photogrammetry metrics for classification analysis was less successful. Fuel types, species, and plant types were less confused when differences detectable by photogrammetry existed. For example, sparse vegetation and litter fuel types (Fuel Types 8 and 9), the most abundant fuel types, were relatively more separable than other fuel types, as indicated by higher numbers of significant pairwise Mann–Whitney tests (Table 5); greater separability was caused by the relatively shallower fuelbed depths of these fuel types (Table 2), which were successfully detected by photogrammetry. ANDVIR was more separable than other species (Tables 4 and 7) because photogrammetric points and derived metrics of ANDVIR tended to be higher than those of other species. Similarly, photogrammetric points and derived metrics from shrubs tended to be higher than those of other plant types. Species and plant types might have been better separated if data had been gathered at a different time of year that maximized species uniqueness in morphology and color, i.e., in the spring and fall when most flowering occurs in these systems. Producing metrics from RGB values of the 2D digital photographs, opposed to using RGB values at photogrammetric points as we did here, might provide additional information that could potentially increase separability among fuel types, species, and plant types, and is a possible consideration for future research.

CONCLUSION

Our results indicate that close-range photogrammetry has potential for yielding fine-scale measurements of understory fuels and plants; however, disagreement between photogrammetry and point-intercept height data and low overall classification accuracies leave room for improvement. We found poor to moderate agreement between close-range photogrammetry heights and field-measured fuelbed depths. Fuel types, plant species, and plant types were often separable in terms of photogrammetry-derived metrics; however, overall accuracies were poor, although better than random, when classifying fuel types, plant species, and plant types using the same metrics.

Close-range photogrammetry has the potential to improve on point-intercept techniques by generating more and less subjective height measurements. Other advantages of close-range photogrammetry are the ability to create a permanent record of understory vegetation and fuels that would support retrospect analyses and for the calibration of human interpreters. As such, photogrammetry might be a highly feasible alternative to point-intercept techniques for characterizing fine-scale understory fuels and plants and should be explored further.

FUNDING

This research was funded by the Strategic Environmental Research and Development Program (#RC-2243).

ORCID

Joseph J. O'Brien http://orcid.org/0000-0003-3446-6063

REFERENCES

Andersen, H.E., McGaughey, R.J., and Reutebuch, S.E. 2005. "Estimating forest canopy fuel parameters using LIDAR data." *Remote Sensing of Environment*, Vol. 94(No. 4): pp. 441–449.

Baltsavias, E.P. 1999. "A comparison between photogrammetry and laser scanning." *ISPRS Journal of Photogrammetry and Remote Sensing*, Vol. 54(No. 2–3): pp. 83–94.

Bohlin, J., Wallerman, J., and Fransson, J.E.S. 2012. "Forest variable estimation using photogrammetric matching of digital aerial images in combination with a high-resolution DEM." *Scandinavian Journal of Forest Research*, Vol. 27(No. 7): pp. 692–699.

Breiman, L. 2001. "Random forests." *Machine Learning*, Vol. 45(No. 1): pp. 5–32.

Caliński, T., and Harabasz, J. 1974. "A dendrite method for cluster analysis." *Communications in Statistics*, Vol. 3(No. 1): pp. 1–27.

Charrad, M., Ghazzali, N., Boiteau, V., and Niknafs, A. 2014. "NbClust: An R package for determining the relevant number of clusters in a data set." *Journal of Statistical Software*, Vol. 61 (No. 6): pp. 1–36.

Dandois, J.P., and Ellis, E.C. 2013. "High spatial resolution three-dimensional mapping of vegetation spectral dynamics using computer vision." *Remote Sensing of Environment*, Vol. 136: pp. 259–276.

Dassot, M., Constant, T., and Fournier, M. 2011. "The use of terrestrial LiDAR technology in forest science: application fields, benefits and challenges." *Annals of Forest Science*, Vol. 68(No. 5): pp. 959–974.

Dimitrakopoulos, A.P. 2002. "Mediterranean fuel models and potential fire behaviour in Greece." *International Journal of Wildland Fire*, Vol. 11(No. 2): pp. 127–130.

Gower, J.C. 1971. "A general coefficient of similarity and some of its properties." *Biometrics*, Vol. 27(No. 4): pp. 857–871.

Hiers, J.K., O'Brien, J.J., Mitchell, R.J., Grego, J.M., and Loudermilk, E.L. 2009. "The wildland fuel cell concept: an approach to characterize fine-scale variation in fuels and fire in frequently burned longleaf pine forests." *International Journal of Wildland Fire*, Vol. 18(No. 3): pp. 315–325.

Hudak, A.T., Crookston, N.L., Evans, J.S., Hall, D.E., and Falkowski, M.J. 2008. "Nearest neighbor imputation of species-level, plot-scale forest structure attributes from LiDAR data." *Remote Sensing of Environment*, Vol. 112(No. 5): pp. 2232–2245.

Hudak, A.T., Evans, J.S., and Smith, A.M.S. 2009. "LiDAR utility for natural resource managers." *Remote Sensing*, Vol. 1(No. 4): pp. 934–951.

Hudak, A.T., Strand, E.K., Vierling, L.A., Byrne, J.C., Eitel, J., Martinuzzi, S., and Falkowski, M.J. 2012. "Quantifying aboveground forest carbon pools and fluxes from repeat LiDAR surveys." *Remote Sensing of Environment*, Vol. 123: pp. 25–40.

Hudak, A.T., Dickinson, M.B., Bright, B.C., Kremens, R.L., Loudermilk, E.L., O'Brien, J.J., Hornsby, B.S., and Ottmar, R.D. 2015. "Measurements relating fire radiative energy density and surface fuel consumption – RxCADRE 2011 and 2012." *International Journal of Wildland Fire*, Vol. 25(No. 1): pp. 25–37.

Isenburg, M. 2015. *LAStools – efficient tools for LiDAR processing, version 150304*, http://lastools.org. Software downloaded March 2015.

James, M.R., and Robson, S. 2012. "Straightforward reconstruction of 3D surfaces and topography with a camera: Accuracy and geoscience application." *Journal of Geophysical Research – Earth Surface*, Vol. 117(No. F03017): pp. 1–17.

Keane, R.E. 2013. "Describing wildland surface fuel loading for fire management: a review of approaches, methods and systems." *International Journal of Wildland Fire*, Vol. 22(No. 1): pp. 51–62.

Kirkman, L.K., Mitchell, R.J., Helton, R.C., and Drew, M.B. 2001. "Productivity and species richness across an environmental gradient in a fire-dependent ecosystem." *American Journal of Botany*, Vol. 88(No. 11): pp. 2119–2128.

Leberl, F., Isachara, A., Pock, T., Meixner, P., Gruber, M., Scholz, S., and Wiechert, A. 2010. "Point Clouds: LiDAR versus 3D Vision." *Photogrammetric Engineering & Remote Sensing*, Vol. 76(No. 10): pp. 1123–1134.

Lefsky, M.A., Cohen, W.B., Parker, G.G., and Harding, D.J. 2002. "LiDAR remote sensing for ecosystem studies." *BioScience*, Vol. 52(No. 1): pp. 19–30.

Lisein, J., Pierrot-Deseilligny, M., Bonnet, S., and Lejeune, P. 2013. "A photogrammetric workflow for the creation of a forest canopy height model from small unmanned aerial system imagery." *Forests*, Vol. 4: pp. 922–944.

Loudermilk, E.L., Hiers, J.K., O'Brien, J.J., Mitchell, R.J., Singhania, A., Fernandez, J.C., Cropper, W.P., and Slatton, K.C. 2009. "Ground-based LIDAR: a novel approach to quantify fine-scale fuelbed characteristics." *International Journal of Wildland Fire*, Vol. 18(No. 6): pp. 676–685.

Loudermilk, E.L., O'Brien, J.J., Mitchell, R.J., Cropper, W.P., Hiers, J.K., Grunwald, S., Grego, J., and Fernandez-Diaz, J.C. 2012. "Linking complex forest fuel structure and fire behaviour at fine scales." *International Journal of Wildland Fire*, Vol. 21(No. 7): pp. 882–893.

Martinuzzi, S., Vierling, L.A., Gould, W.A., Falkowski, M.J., Evans, J.S., Hudak, A.T., and Vierling, K.T. 2009. "Mapping snags and understory shrubs for a LiDAR-based assessment of wildlife habitat suitability." *Remote Sensing of Environment*, Vol. 113(No. 12): pp. 2533–2546.

Miller, D.R., Quine, C.P., and Hadley, W. 2000. "An investigation of the potential of digital photogrammetry to provide measurements of forest characteristics and abiotic damage." *Forest Ecology and Management*, Vol. 135(No. 1): pp. 279–288.

Mitchell, R.J., Hiers, J.K., O'Brien, J., and Starr, G. 2009. "Ecological forestry in the southeast: understanding the ecology of fuels." *Journal of Forestry*, Vol. 107(No. 8): pp. 391–397.

Murphy, G. 2008. "Determining stand value and log product yields using terrestrial lidar and optimal bucking: a case study." *Journal of Forestry*, Vol. 106(No. 6): pp. 317–324.

Mutlu, M., Popescu, S.C., Stripling, C., and Spencer, T. 2008. "Mapping surface fuel models using LiDAR and multispectral data fusion for fire behavior." *Remote Sensing of Environment*, Vol. 112(No. 1): pp. 274–285.

Mutlu, M., Popescu, S.C., and Zhao, K. 2008. "Sensitivity analysis of fire behavior modeling with LiDAR-derived surface fuel maps." *Forest Ecology and Management*, Vol. 256(No. 3): pp. 289–294.

Myers, R.L., and Ewel, J.J. (Editors). 1990. *Ecosystems of Florida*. Gainesville, FL: University Press of Florida.

Næsset, E. 2002. "Determination of mean tree height of forest stands by digital photogrammetry." *Scandinavian Journal of Forest Research*, Vol. 17(No. 5): pp. 446–459.

Noss, R.F. 1989. "Longleaf pine and wiregrass: Keystone components of an endangered ecosystem." *Natural Areas Journal*, Vol. 9(No. 4): pp. 211–213.

Nouwakpo, S.K., Weltz, M.A., and McGwire, K. 2015. "Assessing the performance of structure-from-motion photogrammetry and terrestrial LiDAR for reconstructing soil surface microtopography of naturally vegetated plots." *Earth Surface Processes and Landforms*, Vol. 41(No. 3): pp. 308–322.

O'Brien, J.J., Hiers, J.K., Callaham, M.A., Mitchell, R.J., and Jack, S.B. 2008. "Interactions among overstory structure, seedling life-history traits, and fire in frequently burned neotropical pine forests." *AMBIO: A Journal of the Human Environment*, Vol. 37: pp. 542–547.

O'Brien, J., Loudermilk, E., Hornsby, B., Pokswinski, S., Hudak, A., Hiers, J., Bright, B., Rowell, E., and Dexter, S. 2016. "Canopy derived fuels drive patterns of in-fire energy release and understory plant mortality in a longleaf pine (*Pinus palustris*) sandhill in Northwest Florida, USA." *Canadian Journal of Remote Sensing*, Vol. 42(No. 5): pp. 489–500.

Paine, D.P., and Kiser, J.D. 2012. *Aerial photography and image interpretation* (3rd ed.). Hoboken, NJ: John Wiley & Sons.

Pontius, R.G. and Santacruz, A. 2015. "*diffeR: Metrics of Difference for Comparing Pairs of Maps*. R package version 0.0–4." http://CRAN.R-project.org/package=diffeR. Accessed 7 July 2016.

R Core Team. 2014. *R: A language and environment for statistical computing*. Vienne, Austria: R Foundation for Statistical Computing, http://www.R-project.org/. Software downloaded July 2014.

Riano, D., Chuvieco, E., Ustin, S.L., Salas, J., Rodriguez-Perez, J.R., Ribeiro, L.M., Viegas, D.X., Moreno, J.M., and Fernandez, H. 2007. "Estimation of shrub height for fuel-type mapping combining airborne LiDAR and simultaneous color infrared ortho imaging." *International Journal of Wildland Fire*, Vol. 16(No. 3): pp. 341–348.

Riano, D., Meier, E., Allgower, B., Chuvieco, E., and Ustin, S.L. 2003. "Modeling airborne laser scanning data for the spatial generation of critical forest parameters in fire behavior modeling." *Remote Sensing of Environment*, Vol. 86(No. 2): pp. 177–186.

Rowell, E., and Seielstad, C. 2012. "Characterizing grass, litter, and shrub fuels in longleaf pine forest pre- and post-fire using terrestrial lidar."Paper presented at Proceedings of SilviLaser 2012, Vancouver, B.C., Canada, September 16–19, 2012.

Ruefenacht, B., Finco, M.V., Nelson, M.D., Czaplewski, R., Helmer, E.H., Blackard, J. A., Holden, G.R., et al. 2008. "Conterminous U.S. and Alaska forest type mapping using forest inventory and analysis data." *Photogrammetric Engineering & Remote Sensing*, Vol. 74(No. 11): pp. 1379–1388.

Seielstad, C.A., and Queen, L.P. 2003. "Using airborne laser altimetry to determine fuel models for estimating fire behavior." *Journal of Forestry*, Vol. 101(No. 4): pp. 10–15.

Slama, C.C., Theurer, C., and Henriksen, S.W. (Editors). 1980. *Manual of Photogrammetry*. Falls Church, VA: American Society of Photogrammetry.

Slatton, K.C., Coleman, M., Carter, W., Shrestha, R., and Sartori, M. 2004. "Control methods for merging alsm and ground-based laser point clouds acquired under forest canopies." In *Proceedings of 4th International Asia-Pacific Environmental Remote Sensing Symposium*, edited by M. Bevis, Y. Shoji, and S. Businger, pp. 96–103. Honolulu, Hawaii: SPIE.

Smart, L.S., Swenson, J.J., Christensen, N.L., and Sexton, J.O. 2012. "Three-dimensional characterization of pine forest type and red-cockaded woodpecker habitat by small-footprint, discrete-return LiDAR." *Forest Ecology and Management*, Vol. 281: pp. 100–110.

Spurr, S.H. 1960. *Photogrammetry and Photo-Interpretation: With a Section on Applications to Forestry*. New York, NY: Ronald Press Co.

United States Air Force. 2010. *Integrated Natural Resources Management Plan (INRMP) for Eglin Air Force Base*. Shalimar, FL: Science Applications International Corporation (SAIC).

United States Forest Service. 1975. *Photointerpretation Guide for Forest Resource Inventories*. Washington, DC: United States Department of Agriculture, Forest Service.

Vierling, K.T., Vierling, L.A., Gould, W.A., Martinuzzi, S., and Clawges, R.M. 2008. "LiDAR: shedding new light on habitat characterization and modeling." *Frontiers in Ecology and the Environment*, Vol. 6(No. 2): pp. 90–98.

Westoby, M.J., Brasington, J., Glasser, N.F., Hambrey, M.J., and Reynolds, J.M. 2012. "'Structure-from-Motion' photogrammetry: A low-cost, effective tool for geoscience applications." *Geomorphology*, Vol. 179: pp. 300–314.

Wiggers, M.S., Kirkman, L.K., Boyd, R.S., Hiers, J.K. 2013. "Fine-scale variation in surface fire environment and legume germination in the longleaf pine ecosystem." *Forest Ecology and Management*, Vol. 310: pp. 54–63.

Zagalikis, G., Cameron, A.D., and Miller, D.R. 2005. "The application of digital photogrammetry and image analysis techniques to derive tree and stand characteristics." *Canadian Journal of Forest Research*, Vol. 35(No. 5): pp. 1224–1237.